CORA Cork Open Research Archive
Cartlann Taighde Oscailte Chorcaí

Title	Precursor concentration and substrate effects on high rate dip-coated vanadium oxide thin films.
Authors	Glynn, Colm;Aureau, Damien;O'Hanlon, Sally;Daly, Luke;Geaney, Hugh;Collins, Gillian;Etcheberry, Arnaud;O'Dwyer, Colm
Publication date	2015-05-01
Original Citation	Glynn, C., Aureau, D., O'Hanlon, S., Daly, L., Geaney, H., Collins, G., Etcheberry, A. and O'Dwyer, C. (2015) 'Precursor Concentration and Substrate Effects on High Rate Dip-Coated Vanadium Oxide Thin Films', ECS Transactions, 64(42), pp. 1-9. doi: 10.1149/06442.0001ecst
Type of publication	Article (peer-reviewed)
Link to publisher's version	http://ecst.ecsdl.org/content/64/42/1.abstract - 10.1149/06442.0001ecst
Rights	© 2015 ECS - The Electrochemical Society
Download date	2026-10-07 10:19:52
Item downloaded from	https://hdl.handle.net/10468/6284

UCC
University College Cork, Ireland
Coláiste na hOllscoile Corcaigh

Precursor Concentration and Substrate Effects on High Rate Dip-Coated Vanadium Oxide Thin Films

Colm Glynn[1,2], Damien Aureau[3], Sally O'Hanlon[1], Luke Daly[1], Hugh Geaney[1,2], Gillian Collins[1,2], Arnaud Etcheberry[3], and Colm O'Dwyer[1,2]

[1]Department of Chemistry, University College Cork, Cork, Ireland
[2]Micro & Nanoelectronics Centre, Tyndall National Institute, Lee Maltings, Cork, Ireland
[3]Centre de Spectroscopie, Institut Lavoisier de Versailles, Université de Versailles Saint Quentin-en-Yvelines, 78035 Versailles Cedex, France

Uniform thin films of vanadium pentoxide were dip-coated from a high-concentration vanadium oxytriisopropoxide precursor which is shown to be resistant to the dewetting processes which can form surface pinhole defects. Through appropriate withdrawal speed choice, the thin films have a smooth uniform surface morphology with a low rms roughness of <1 nm in both their amorphous and crystallized states. The structure of the thin films follows that of bulk vanadium pentoxide but in a nanostructured form. The deposition methods shown can be applied to prepare thin films upon a variety of different substrates and other alkoxide based metal oxide materials.

Introduction

The use of metal oxide thin films continues to be of high importance for in modern technologies. New applications of these thin films for the electronic,[1] energy storage,[2] optoelectronic[3, 4] and photovoltaic[5] industries are researched each year. With an increased range of potential applications, a rapid deposition of thin films over large areas is required. Solution based processing techniques can fill this need. Techniques such as spin- and dip-coating are capable of depositing thin films over large areas in a short time. Unlike other deposition methods that require large processing equipment such as sputtering or physical/chemical vapor (PVD, CVD) methods, spin- and dip-coating methods are cost-effective and have a long history within industry.

While the sample throughput for solution processed techniques can be higher than that of other deposition techniques, certain drawbacks remain. Methods such as sputtering, PVD and CVD have a high level of surface selectivity allowing for intricate areas of substrates to be coated, however, this high selectivity can result in a slow rate of deposition of larger surfaces. The uniform coating of large surfaces at a high throughput is a major strength of solution processed deposition techniques. Different methods can be applied to solution processing techniques to increase thin film uniformity such as; polymer assisted deposition (PAD),[6] catalyst addition[7] and suitable substrate choice.[8]

Thin films of V_2O_5 have seen use in a variety of applications such as energy storage,[2, 9, 10] photovoltaics,[11] intercalation materials[12] and in optoelectronic materials.[13] In our previous work,[14] thin films of V_2O_5 were shown to form surface pinholes under certain deposition conditions. A method of alleviating the formation of pinholes was to increase the ratio between the alkoxide-IPA. This increase in alkoxide concentration increased the formation time of the as-deposited thin films to ensure that the pinholes did not have sufficient time to dewet and form the pinholes.

In this work thin films of vanadium pentoxide (V_2O_5) were deposited from a high-concentration alkoxide based precursor through dip-coating. The goal of this work is to show the behavior of the thin films formed from this precursor on a variety of substrates and what methods can be used to retain uniformity of the thin film surface. The thin film surface morphology, structure and optical characteristics were studied to ascertain the effect that changes to the precursor had on the thin films.

Experimental

Vanadium pentoxide thin films were synthesized from vanadium (V) oxytriisopropoxide [$OV(OCH(CH_3)_2)_3$] purchased from Sigma-Aldrich. The alkoxide was mixed by volume with isopropyl alcohol (IPA) and deionized water at a ratio of 250:10:1 (IPA : alkoxide : H_2O) to produce a high concentration precursor. To prevent hydrolysis prior to deposition, 4 Å molecular sieves from Sigma-Aldrich were stored within the precursor.

Thin films were deposited onto the surface of a variety of substrates using a PTL-MM01 desktop dip coater. A withdraw rate of between 0.176 mm/s and 2.5 mm/s was used depending upon the substrate deposited upon. The substrates were cleaned using acetone and IPA prior to deposition. To remove any organics present on the surface before and after deposition, the samples were UV-Ozone treated for 30 minutes using a Novascan UV ozone system. Thin film samples were crystallized through thermal treatment in a conventional oven at 300 ^oC for 14 hours.

Scanning electron microscopy analysis was performed on an FEI Quanta 650 FEG high resolution SEM equipped with an Oxford Instruments X-MAX 20 large area Si diffused EDX detector. Images were collected at an operating voltage of 10-20 kV. Atomic force microscopy (AFM) was performed on a Park XE-100 AFM system in non-contact mode with SSS-NCHR enhanced resolution tips. The XY and Z resolutions of the AFM system are ~ 2 nm and ~ 0.05 nm respectively.

Raman scattering spectroscopy was collected on a Renishaw InVia Raman spectrometer using a 514 nm 30 mW laser source. Spectra were collected using a RenCam CCD camera and the beam was focused onto the samples using either a 20x or 50x objective lens. To probe the optical transparency of the samples on transparent substrates, a Thermo Scientific Evolution 60S UV-Visible spectrophotometer was used with a custom sample holder. The UV-Vis transmission spectrum of the samples was examined in the 300 – 1000 nm range under a Xenon light source with an accuracy of ±0.8 nm.

XPS spectra were collected on a Thermo Electron K-Alpha spectrometer using a monochromatic Al Kα X-ray source (1486.6 eV). Core level spectra from 100 scans were referenced to the C1s peak at 284.31 eV. The XPS spectra were processed using a Shirley background correction followed by peak fitting to Voigt profiles. The FWHM were allowed to vary within reasonable value ranges in order to achieve best fit.

Results and Discussion

Alkoxide/IPA Concentration Effects and Pinhole Formation

During dip-coating deposition, it was found that surface pinholes can form due to dewetting of the liquid prior to solidification of the thin film.[14] The methods outlined previously for halting the formation of the thin films were either to incorporate PAD techniques or to increase the alkoxide/IPA concentration ratio. The thin films studied in this work are a result of the latter technique.

The AFM surface images of the as-deposited stoichiometric V_2O_5 thin films on Au and ITO substrates with pinholes formed on the surface are shown in Fig. 1 (a). The type of pinhole formed was found to be substrate dependent and were subject to the surface energy and roughness. On Au substrates, the pinholes formed had a low diameter and were scattered throughout the surface. On ITO, the pinholes were larger and irregularly shaped. The average rms roughness of the thin films with pinholes present on the Au and ITO substrates shown are 1.86 nm and 0.362 nm respectively. The pinholes result in increased surface roughness which would be detrimental for applications for which surface uniformity was important and where pinholes would increase the risk of a short circuit, phase mixing, or alterations in optical absorption characteristics, such as in photovoltaic devices.

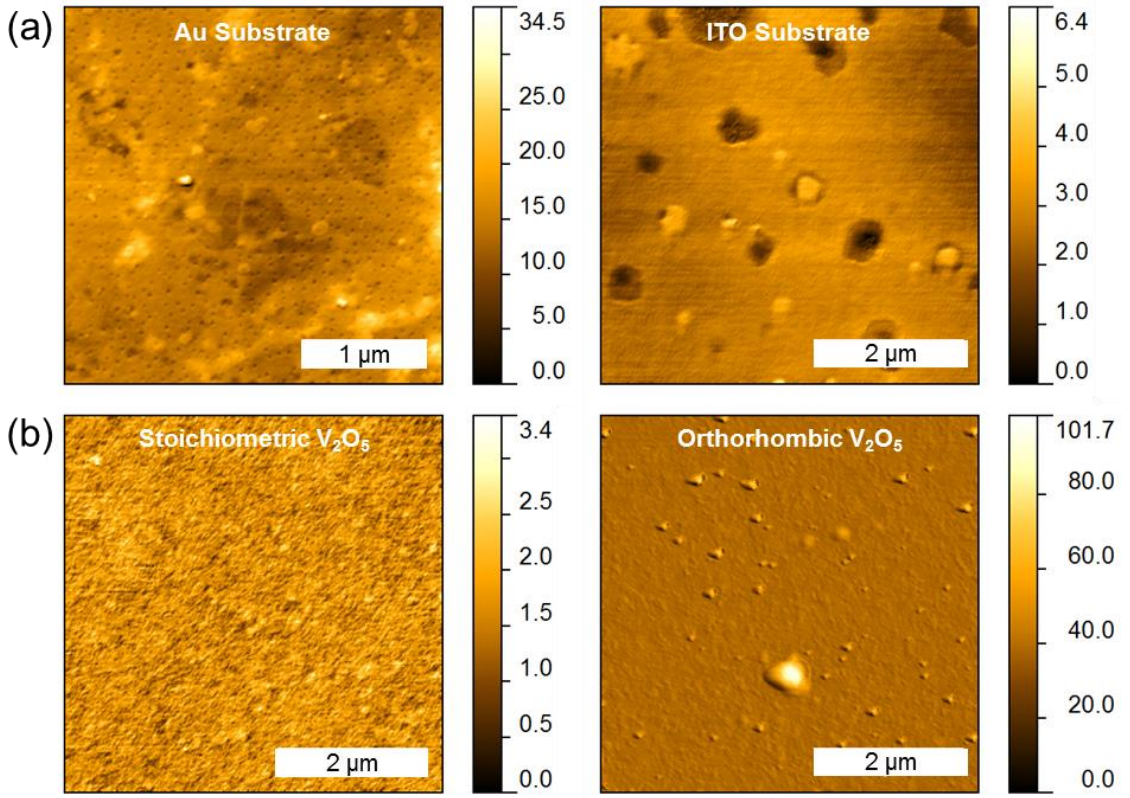

Figure 1. AFM surface images of (a) as-deposited stoichiometric V_2O_5 thin films deposited on Au and ITO substrates showing the formation of pinholes, (b) as-deposited stoichiometric V_2O_5 and heat-treated orthorhombic V_2O_5 thin films on ITO substrate deposited from a high concentration precursor.

Surface AFM images of as-deposited stoichiometric and heat-treated orthorhombic V_2O_5 thin films dip-coated from a high concentration precursor are shown in Fig. 1 (b). The presence of pinholes are not found on the surface of thin films deposited from the higher concentration precursor. The pinholes do not form due to the higher concentration of the precursor resulting in a decreased hydrolyzation and gelation time of the liquid thin film, therefore the mechanism controlling the dewetting which forms the pinholes does not have sufficient time to propagate.

The rms roughness of thin films formed without pinholes predictably decreases. The as-deposited rms roughness for the stoichiometric V_2O_5 thin films is measured to be less than 0.1 nm. After thermal treatment the now orthorhombic V_2O_5 thin films increase to a roughness of 0.92 nm. The increase in roughness after crystallisation is a result of the

densification of the thin film and the formation of small crystallites on the surface as seen in Fig. 1 (b).

High Precursor Concentration Thin Films

Surface SEM images of the as-deposited and thermal treated V_2O_5 thin films are shown in figure 2. Three regions of the thin films formed from the high concentration precursor are shown in the SEM images for comparison. There is a distinct interface between the ITO substrate and the V_2O_5 thin film. The non-linear interface between the films is due to viscous drag within the liquid thin film during deposition. The dragging of the liquid thin film is most apparent at this interface, the SEM images of the main body of the as-deposited thin film shown in Fig. 2 (a) have a smooth surface morphology.

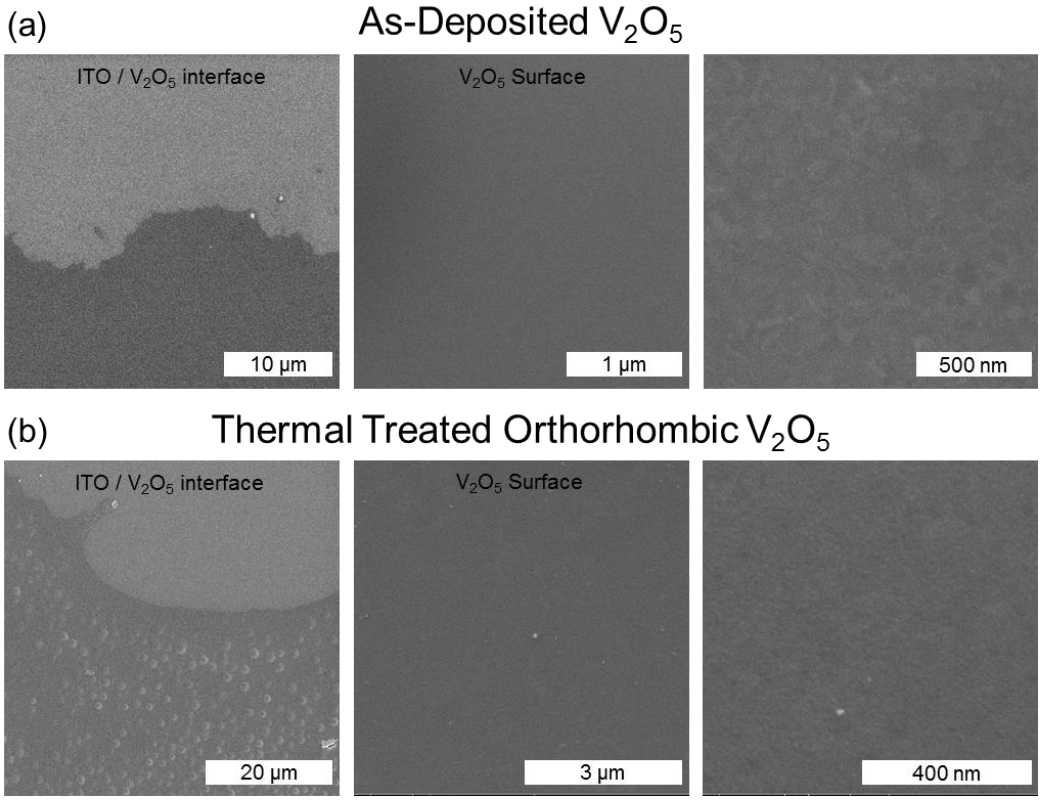

Figure 2. Surface SEM images different regions for (a) as-deposited stoichiometric V_2O_5 and (b) thermal treated orthorhombic V_2O_5 thin films.

The thin films undergo crystallization and densification after thermal treatment of the as-deposited stoichiometric V_2O_5 to orthorhombic V_2O_5 thin films. The densification of the thin films can result in contraction and surface cracking at the ITO/V_2O_5 interface region as seen in Fig. 2 (b) as well as the formation of a larger number of surface crystallites. The surface cracking is confined to the interface region and does not propagate throughout the thin film. Figure 2 (b) shows images of regions further within the thin film which show a continuous thin film with some surface crystallites which form after thermal treatment as discussed previously.

Thin films were prepared from the higher concentration precursor to alleviate the formation of pinholes on the surface. The thin films formed from this high concentration precursor lack the pinholes that are present in those from the low concentration precursor. While the surface is smoother in the high concentration thin film, their thickness is also greater. This thickness increase is to be expected with an increase in alkoxide/IPA concentration. The thickness of thin films deposited from the low concentration and high concentration precursors is ~13-15 nm and ~36-40 nm per dip coated layer respectively.

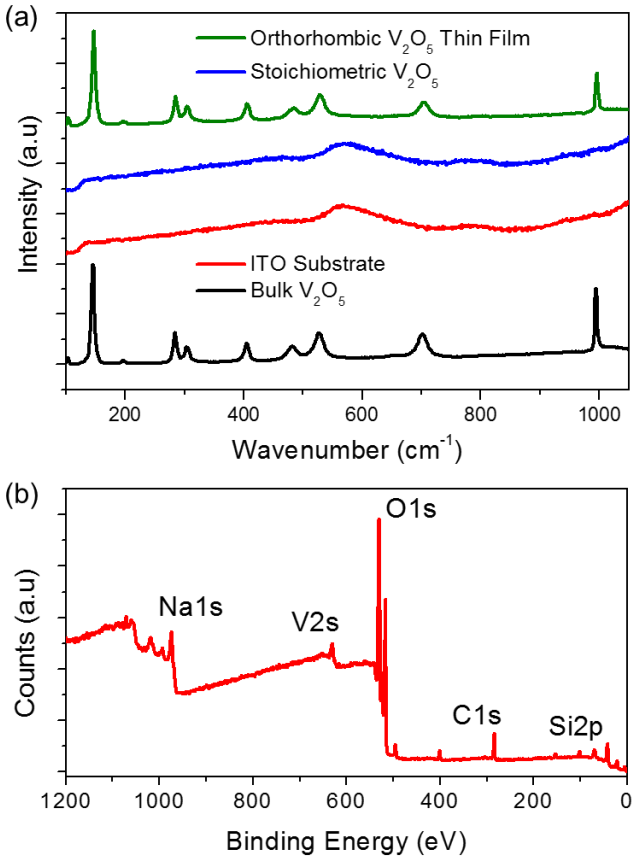

Figure 3. (a) Raman scattering spectroscopy of bulk V_2O_5, ITO substrate, as-deposited stoichiometric V_2O_5 thin film and thermal treated orthorhombic V_2O_5 thin film. (b) XPS measurement of stoichiometric V_2O_5 thin film on a borosilicate glass substrate prior to heat-treatment.

Raman scattering spectroscopy was performed on the stoichiometric and orthorhombic V_2O_5 thin films shown in Fig. 3 (a). Raman scattering spectra were also taken of bulk V_2O_5 and the ITO substrate for comparison. The characteristic V_2O_5 Raman vibrational modes are well known in the literature.[15, 16] The Raman mode located at 145 cm^{-1} is associated with the bilayer shearing of the V_2O_5 structure, this mode is indicative to the layering of the stacked V_2O_5 layers. The V=O mode at ~993 cm^{-1} is related to the mixed valency of V^{4+}/V^{5+} within the material.[12, 17, 18] The presence and lack of red or blue shifting of the 145 cm^{-1} and the V=O mode in the thin films Raman spectra in Fig. 3 (a) shows that the V_2O_5 thin film structure is the same as that of a bulk material but in a nanostructured thin film morphology.

The Raman scattering spectra of both the ITO substrate and the ITO substrate with an as-deposited stoichiometric V_2O_5 thin film are also shown in Fig. 3 (a). There are no

definitive peaks associated with either the ITO substrate or the stoichiometric V_2O_5. The lack of well-defined peaks is due to the non-crystalline nature of the thin films. The as-deposited V_2O_5 is formed as amorphous flakes of stoichiometric V_2O_5 during hydrolysis of the liquid precursor and sets into a thin film form. These amorphous flakes are then crystallized during thermal treatment to form orthorhombic V_2O_5.

Raman scattering was unable to determine the presence of V_2O_5 on the surface of the as-deposited stoichiometric V_2O_5 thin films. An XPS measurement of an as-deposited thin film of V_2O_5 on a glass substrate was performed as shown in Fig. 3 (b). An amorphous stoichiometric thin film of V_2O_5 was determined to be present on the substrate prior to thermal treatment. Small amounts of Si and Na were also found and are attributed to the borosilicate glass substrate.

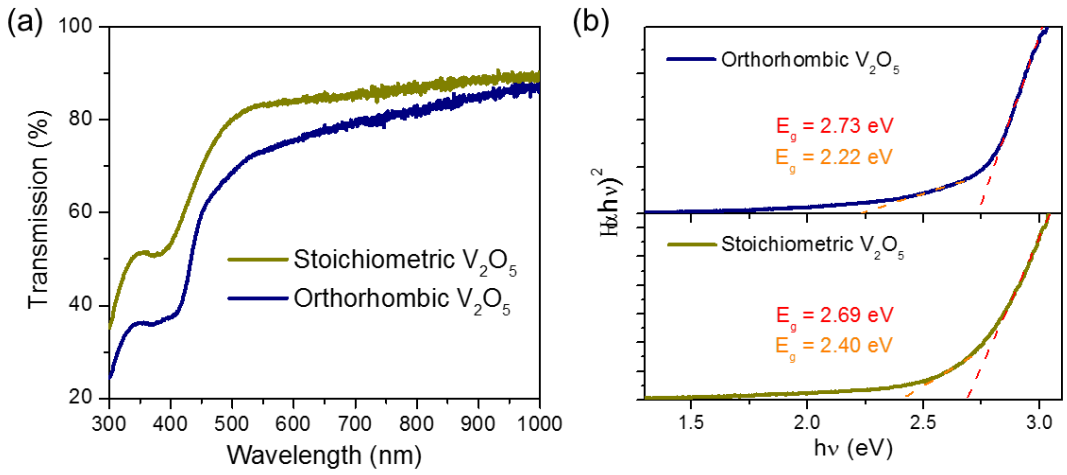

Figure 4. (a) UV-Vis transmission spectroscopy of as-deposited stoichiometric V_2O_5 and orthorhombic V_2O_5 thin films. (b) Modified Davis-Mott relationship analysis performed to calculate E_g of the stoichiometric and orthorhombic V_2O_5 thin films through a Tauc plot.

The optical transmission profile of the V_2O_5 thin films were probed in the UV-Vis 300-1000 nm range. The UV-Vis transmission spectrum for the stoichiometric and orthorhombic V_2O_5 thin films are shown in Fig. 4 (a). A decrease in the transmitted light after crystallization is found for the V_2O_5 thin films. The decrease is attributed to an increase in light scattering and reflection by the thin film. This increase in scattered and reflected light is attributed to the densification of the thin film during the crystallization process. The scattered light absorption edge decreases in wavelength after crystallization which is attributed to a decrease in the optical bandgap of the thin film due to the change from stoichiometric to orthorhombic V_2O_5.

Through the use of a modified Davis-Mott relation, the effective optical bandgap (E_g) of the V_2O_5 thin films can be approximated from a UV-Vis spectrum using a Tauc plot.[19] The corresponding Tauc plot for the stoichiometric and orthorhombic V_2O_5 thin films is shown in Fig. 4 (b). The value of E_g can be calculated by extrapolating the linear region of the graph to $[\alpha h\omega]^2 = 0$. For both the stoichiometric and orthorhombic V_2O_5 thin films, there are two distinct linear regions above the Urbach tail. The region denoted by the orange dashed line in Fig. 4 (b) shows the decrease in the Eg, from 2.40 to 2.22 eV, expected through the shifting of the absorption edge of the UV-Vis transmission spectrum. The E_g of the second region is attributed to absorptions and light scattering due to morphology changes and the presence of other VO phases which were not significant enough to be found using other analysis techniques.

High Concentration Thin Films on Different Substrates

Using the high concentration precursor and dip-coating method outlined above, thin films of V_2O_5 can be deposited upon a variety of substrates. When depositing upon a new substrate, different factors must be taken into account for depositing a uniform thin film. The surface of the new substrate must be examined so that the deposition procedures can be adjusted to form a high grade uniform thin film.

Changes in surface roughness is a particularly important aspect when considering a new substrate. When a substrate has a high or low surface roughness, there can be significant changes in the hydrophobicity of that surface, which must be factored into the deposition methods. A hydrophobic or hydrophilic surface would require changes to the dip coating rate and/or in extreme cases require a pre-treatment in order for a uniform film to be deposited.

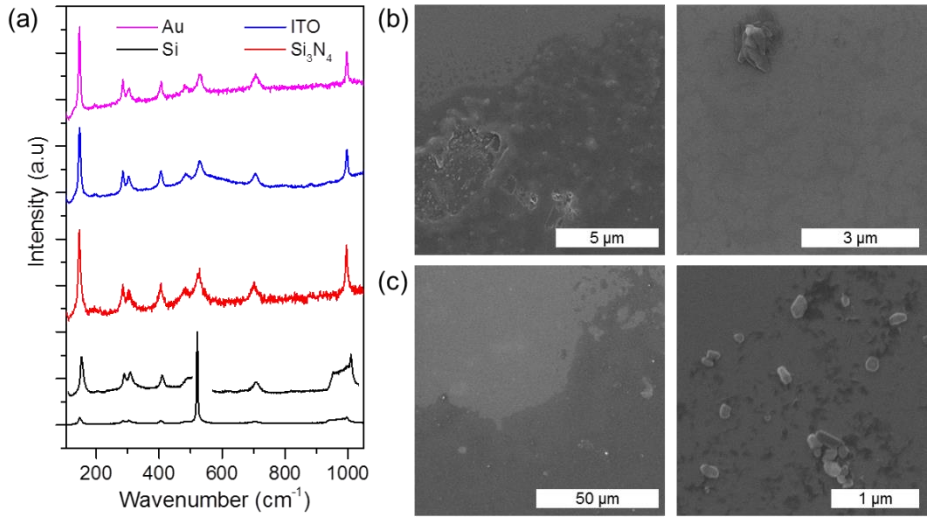

Figure 5. (a) Raman scattering spectroscopy of V_2O_5 thin films deposited upon different substrates. The Raman vibrational modes show the formation of orthorhombic V_2O_5 thin films upon each substrate after thermal treatment. (b, c) SEM images of as-deposited V_2O_5 thin films dip coated at two withdrawal rates, 0.167 mm/s and 2.5 mm/s respectively.

The Raman scattering spectroscopy spectra for thermal treated V_2O_5 thin films deposited on ITO, Au, Si and Si_3N_4 substrates are shown. The Raman scattering spectra show that on each of the substrates, orthorhombic V_2O_5 is formed after thermal treatment. Each of these substrates have a different surface roughness and hydrophobicity and required a change in deposition procedures, namely. The dip coating speed for the thin films deposited on the Au substrate was kept the same as that on ITO due to their surface roughness being comparable.

The effect of an excessively high (2.5 mm/s) withdrawal speed on a Si substrate is shown in Fig. 5 (b). The surface morphology varies due to the effects of the high withdrawal rate on the liquid film during deposition. At higher withdrawal rates, there is increased drainage of the liquid thin film prior to hydrolysis resulting in an uneven coating and the presence of regions where surface inhomogeneities occur.

The effect of a low (0.167 mm/s) withdrawal speed on the Si substrate differs to that of the high speed. At a low withdrawal speed, the hydrolysis occurs close to the meniscus of the alkoxide based precursor. The meniscus has an increased effect on the surface of dip coated thin films at lower withdrawal speeds.[20] For the thin films deposited at 0.167 mm/s shown in Fig. 5 (c), the effect of the slow dip coating results in the formation of clumps of

amorphous V_2O_5 material on the surface. The surface roughness of the thin films is increased due to the clumps, resulting in a non-uniform thin film surface.

When depositing thin films onto a new substrate, the optimal withdrawal rate for forming a uniform and constant morphology must be determined. As discussed above, the substrate surface plays a major role in choosing the withdrawal rate. Experimentally, the optimum rate can be found by depositing thin films at a variety of rates to determine the range where the desired morphology is attained. Future methods may include modelling[21] which utilizes current research into dip-coating of thin films. A correctly calibrated model would enable matching of different precursors and substrates to each other for preparing thin films of desired morphologies and structures.

Conclusions

Thin films formed from a high-concentration V_2O_5 alkoxide-IPA precursor were prepared through dip-coating on a variety of substrates. Previously, this precursor was used to alleviate the formation of pinhole defects on the surface of thin films. The thin films were found to be thicker than those prepared from the low-concentration precursor, however, they did not allow the formation of pinholes on the surface. The surface morphology of the thin films were found to have a low rms roughness of <1 nm for both the as-deposited stoichiometric and heat-treated orthorhombic V_2O_5 films.

The effect of withdrawal speed during dip-coating was found to be an important attribute of the deposition. Both a high and low withdrawal rate resulted in discontinuities of the thin film surface. These discontinuities can be alleviated through experimentation to find the optimum withdrawal speed which results in a uniform surface morphology. The dip-coating deposition technique outlined in this work provides a rapid, up-scalable technique for preparing uniform amorphous and crystalline V_2O_5 thin films. The processes involved can be applied to many different alkoxide and carboxylate based metal oxide precursors.

Acknowledgments

C.G. acknowledges the support of the Irish Research Council under award RS/2011/797. C.O.D. acknowledges support from the UCC Strategic Research Fund, and from the Irish Research Council New Foundations Award. This work was also supported by SFI under the National Access Programme (NAP 417).

References

1. P. K. Nayak, J. A. Caraveo-Frescas, Z. Wang, M. N. Hedhili, Q. X. Wang, H. N. Alshareef, *Sci. Rep.*, **4**, (2014).
2. G. Gershinsky, H. D. Yoo, Y. Gofer, D. Aurbach, *Langmuir*, **29**, 10964 (2013).
3. T. Paik, S.-H. Hong, E. A. Gaulding, H. Caglayan, T. R. Gordon, N. Engheta, C. R. Kagan, C. B. Murray, *ACS Nano*, (2013).
4. Z. Mao, W. Wang, Y. Liu, L. Zhang, H. Xu, Y. Zhong, *Thin Solid Films*, **558**, 208 (2014).
5. J. Boucle, P. Ravirajan, J. Nelson, *J Mater Chem*, **17**, 3141 (2007).
6. T. Schneller, R. Waser, M. Kosec, D. Payne, *Chemical Solution Deposition of Functional Oxide Thin Films*. p 796, Springer, London (2013).
7. A. Carretero-Genevrier, M. Gich, L. Picas, J. Gazquez, G. L. Drisko, C. Boissiere, D. Grosso, J. Rodriguez-Carvajal, C. Sanchez, *Science*, **340**, 827 (2013).
8. A. Carretero-Genevrier, G. L. Drisko, D. Grosso, C. Boissiere, C. Sanchez, *Nanoscale*, **6**, 14025 (2014).
9. D. McNulty, D. N. Buckley, C. O'Dwyer, *J. Power Sources*, **267**, 831 (2014).
10. D. McNulty, D. N. Buckley, C. O'Dwyer, *J. Electrochem. Soc.*, **161**, A1321 (2014).
11. H. H. Jung, J.-D. Kwon, S. Lee, C. S. Kim, K.-S. Nam, Y. Jeong, K.-B. Chung, S. Y. Ryu, T. Ocak, A. Eray, D.-H. Kim, S.-G. Park, *Appl. Phys. Lett.*, **103**, 073903 (2013).
12. C. Glynn, D. Thompson, J. Paez, G. Collins, E. Benavente, V. Lavayen, N. Yutronic, J. D. Holmes, G. Gonzalez, C. O'Dwyer, *J. Mater. Chem. C*, **1**, 5675 (2013).
13. M. Benmoussa, A. Outzourhit, A. Bennouna, E. L. Ameziane, *Thin Solid Films*, **405**, 11 (2002).
14. C. Glynn, D. Creedon, H. Geaney, J. O'Connell, J. D. Holmes, C. O'Dwyer, *ACS Appl. Mater. Interfaces*, **6**, 2031 (2014).
15. J. Zhu, L. Cao, Y. Wu, Y. Gong, Z. Liu, H. E. Hoster, Y. Zhang, S. Zhang, S. Yang, Q. Yan, P. M. Ajayan, R. Vajtai, *Nano Lett*, (2013).
16. E. Armstrong, M. Osiak, H. Geaney, C. Glynn, C. O'Dwyer, *CrystEngComm*, **16**, 10804 (2014).
17. C. O'Dwyer, V. Lavayen, S. B. Newcomb, M. A. Santa Ana, E. Benavente, G. González, C. M. Sotomayor Torres, *J. Electrochem. Soc.*, **154**, K29 (2007).
18. V. Lavayen, C. O'Dwyer, M. A. Santa Ana, S. B. Newcomb, E. Benavente, G. González, C. M. Sotomayor Torres, *Phys. Status Solidi*, **243**, 3285 (2006).
19. J. Tauc, *The optical properties of solids*. Academic Press, New York (1966).
20. M. Faustini, B. Louis, P. A. Albouy, M. Kuemmel, D. Grosso, *J. Phys. Chem. C*, **114**, 7637 (2010).
21. M. Faustini, D. R. Ceratti, B. Louis, M. Boudot, P.-A. Albouy, C. Boissière, D. Grosso, *ACS Appl. Mater. Interfaces*, **6**, 17102 (2014).